

Measuring the Cosmic Ray Spectrum with Next Generation Neutrino Detectors

Stephan A. Meighen-Berger ^{1,2,*}, Jayden L. Newstead ^{1,3,†} and Louis E. Strigari ^{4,5,‡}

¹*School of Physics, The University of Melbourne, Victoria 3010, Australia* 

²*Center for Cosmology and AstroParticle Physics (CCAPP),*

Ohio State University, Columbus, OH 43210, USA 

³*ARC Centre of Excellence for Dark Matter Particle Physics,*

School of Physics, The University of Melbourne, Victoria 3010, Australia 

⁴*Department of Physics and Astronomy, Texas A&M University, College Station, TX 77843, USA* 

⁵*George P. and Cynthia Woods Mitchell Institute for Fundamental Physics and Astronomy,*

Texas A&M University, College Station, TX 7783, USA 

(Dated: June 8, 2025)

We investigate the capabilities of upcoming kiloton-scale neutrino detectors, such as Hyper-Kamiokande, in determining the primary cosmic ray spectrum. These detectors provide full-sky coverage and long-term monitoring, unlike traditional satellite and balloon experiments that measure cosmic ray flux at specific altitudes and locations. By analyzing the atmospheric neutrino flux generated by cosmic ray interactions, we demonstrate that future detectors can differentiate between various cosmic ray models with high statistical significance, even when accounting for uncertainties in neutrino cross sections and hadronic interactions. We introduce a technique for reconstructing the primary cosmic ray spectrum using neutrino measurements, which reduces the flux uncertainty from approximately 20% to about 7%. We then show that Hyper-K has the potential to increase sensitivity to neutrino oscillation parameters, such as $\sin^2 \theta_{23}$, by a factor of 2. Our results highlight the complementary role of neutrino detectors in cosmic ray physics and their critical importance for precision measurements in particle astrophysics.

I. INTRODUCTION

Next-generation large-scale neutrino detectors such as JUNO [1], Hyper-K [2], and DUNE [3] are poised to significantly advance our understanding of neutrino sources in the \sim MeV energy range, including the Sun, the atmosphere, diffuse supernovae, and potentially individual supernova events. Similarly, upcoming large-volume dark matter detectors will achieve sensitivity to low-energy neutrinos through independent detection channels, enabling complementary studies of these sources [4].

Among these, atmospheric neutrinos [5–11] constitute a critical signal. A precise understanding of the low-energy atmospheric neutrino flux ($E_\nu < 100$ MeV) is crucial for multiple physics goals: probing neutrino oscillations [12–17], mass ordering [18, 19], flavor ratios [20, 21], and it acts as a background in the search for the diffuse supernova neutrino background (DSNB) [1, 22–25], proton decay [1, 2, 26–28] indirect [29–32] and in direct detection searches for dark matter [33–35].

Atmospheric neutrinos originate from cosmic ray (CR) interactions in the Earth’s atmosphere, which produce showers that generate neutrinos as a secondary component. A variety of satellite-, balloon-, and ground-based experiments have directly measured the primary CR proton and helium spectra, including AMS [36], CREAM [37], PAMELA [38], BESS [39], helium: AMS [40], ATIC-2 [41], BESS [39], CREAM [37], PAMELA [38], among others. These measurements are generally well-described by phenomenological and empirical cosmic ray source models, such as HillasGaisser [42], Gaisser-Stanev-Tilav [43], HKKM [44, 45]. Atmospheric

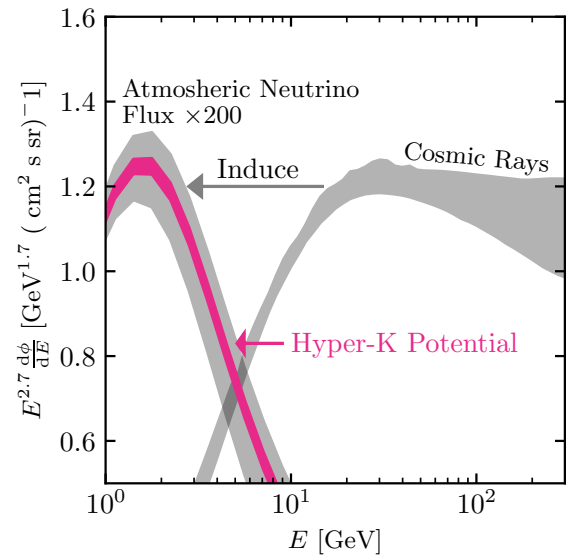


FIG. 1. A sketch of where differences in the primary flux will appear in neutrino data. Shown (in black) are the neutrino fluxes produced when injecting PAMELA, BESS, AMS, or HKKM CR proton. The pink area denotes Hyper-K’s predicted statistical precision when measuring the neutrino flux.

shower simulations, such as HKKM [44, 45], CORSIKA [46], and MCEq [47], are then used to predict the atmospheric neutrino spectrum, for a given primary CR spectrum as input. These spectra are a critical input to *any* neutrino analysis. While [48] previously studied how one can combine different CR data sets to reduce

the uncertainty on the neutrino flux, here we reverse the logic.

With the increasing precision and scale of neutrino detectors, it is timely to investigate how measurements of atmospheric neutrinos can inform phenomenological models of the primary CR spectrum. At the low energies relevant for atmospheric neutrino production, two principal effects on the CR spectrum must be considered: solar modulation [49], which alters the spectrum as particles traverse the heliosphere, and geomagnetic deflection, which imposes a rigidity cut-off that varies with location and direction at the Earth's surface.

Concerning the atmospheric neutrino flux, experiments such as Super-Kamiokande have provided high-statistics measurements [50], constraining neutrino oscillation parameters and even hinting at time variability correlated with cosmic ray modulation. Recent studies have explored the impact of detector location [51] and solar cycle variations [52] on the low-energy atmospheric neutrino flux, highlighting the sensitivity of future detectors to these effects, particularly at higher latitudes.

In this work we evaluate the potential for future experiments to precisely measure the atmospheric neutrino flux, and show how this flux may be used to measure the CR spectrum. Figure 1 sketches out our general approach. We use experimental CR flux measurements (right grey shaded band) to predict the resulting neutrino flux (left grey shaded band) at Hyper-K. We then show that Hyper-K's statistical precision can differentiate between these injected fluxes (pink shaded band).

In Sections II and III we define the primary CR and shower models, respectively, that we use in this analysis. In Section IV, using HyperK as an example, we show how atmospheric neutrinos measurements can directly inform models of primary CR spectra and CR shower physics. Then, in Section VI, we show how this improved knowledge of the models can be leveraged to improve atmospheric neutrino oscillation measurements. Lastly, in Section VII we close with an outlook and concluding remarks.

II. COSMIC RAYS

The atmospheric neutrino flux at energies $E_\nu \leq 100$ GeV is primarily sourced by CRs with energies $E_{\text{CR}} \in [1 \text{ GeV}, 1 \text{ TeV}]$. For simplicity, we assume these CR to be purely composed of protons. Although there is a subleading helium component ($\approx 10\%$ - 20% as measured by AMS [40]), we assume the neutrino spectrum produced from these showers is the same as that produced by protons. Some shower observables, such as the depth of shower maximum X_{max} , the total muonic component of the shower N_μ , and the characteristic width of the shower profile L , do differ between p and He initiated showers [53, 54], for simplicity we do not account for these differences as they do not affect our results.

Here we define three primary CR models to illustrate

the effects that they have on the final neutrino spectrum and the neutrino detectors' capabilities to distinguish between them. We will use the measurements by AMS [36] as a benchmark and compare the neutrino spectra when injecting PAMELA [38] data and the CR model used in HKKM [44, 45]. For low energies ($E_{\text{CR}} < 1 \text{ TeV}$) HKKM uses a proton and helium spectra mainly based on AMS02 [36]. Above 1 TeV the HKKM model is based on CREAM [37], JACEE [55], and RUNJOB [56].

III. NEUTRINO SHOWERS

At the energies of interest, atmospheric neutrinos are primarily produced by sequential decays of pions and muons produced by CR interactions in the upper atmosphere [57–59]. Here we ignore muons produced in electromagnetic showers due to their minimal contribution [60–62]. We simulate the production of neutrinos in the atmosphere using the site-dependent solar-cycle averaged predictions of HKKM11 [44], which agree well with Super-K measurements [63]. For energies below 0.15 GeV (where the HKKM11 predictions stop), we use predictions from [51], which combines FLUKA [64] and CORSIKA [46] to make site-dependent low-energy flux predictions.

To model the effects of different injected CR spectra and hadronic models, we use MCEq [47], which is a cascade-equation [57, 65–67] based simulation tool. We then use the resulting changes predicted by MCEq to rescale the HKKM11 and low-energy atmospheric fluxes. In MCEq we used the hadronic interaction models Sybill 2.3 [68, 69], EPOS-LHC [70], QGSJET-II [71], and DPMJET-III [72, 73] as well as the atmospheric models from CORSIKA (US Standard) [46], and NRLMSISE-00 [74] to assess the uncertainties from the underlying hadronic and atmospheric models. Note [75] has shown that the uncertainties from Hadronic interaction models can be pushed down to $\sim 5\%$ for energies $E_\nu \leq 10$ GeV. This uncertainty is primarily caused by uncertainties from π and K production in the atmosphere [76], while the kaon to pion ratio itself should be irrelevant [42].

IV. MEASUREMENT POTENTIAL

Hyper-K, the successor to Super-K [77], is a cylindrical water-based Cherenkov detector with a fiducial volume of 187 kton [2, 78]. With angular resolution $\sim 10^\circ$ [79] for $p_{e,\mu} = 10$ GeV, detection efficiency $> 80\%$ [63] for CC ν_μ events, and excellent energy resolution $\leq 10\%$ [80–82], this detector will have an order of magnitude more well-reconstructed data than previous generations of detectors for neutrino energies below 10 GeV.

Here we consider atmospheric neutrino CC scattering on oxygen for Hyper-K. To predict the number of atmo-

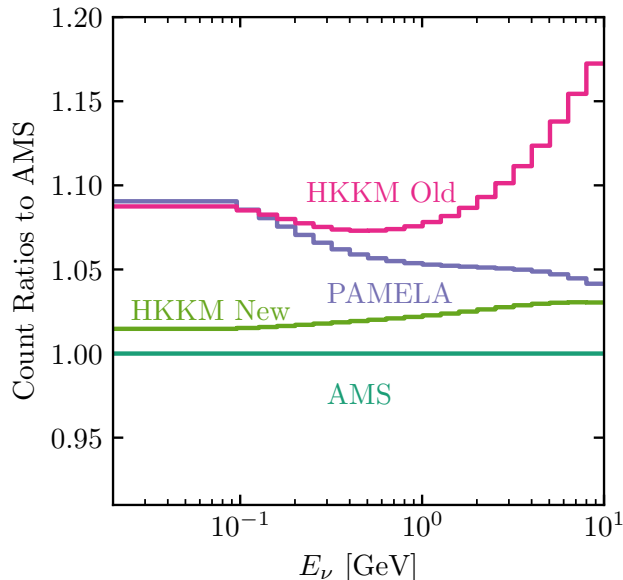


FIG. 2. The resulting neutrino counts compared to the AMS prediction when injecting PAMELA or HKKM data.

spheric events in an energy bin j , we use

$$\mathcal{N}^j = N_t \Delta t \int_{E_j}^{E_{j+1}} dE_\nu \frac{d\Phi}{dE_\nu}(E_\nu) \sigma(E_\nu) \epsilon(E_\nu), \quad (1)$$

where N_t is the number of target atoms (water), ϵ the detection efficiency (80% for Hyper-K), and Δt is the detector livetime. For the exposure, we assume 10 years of livetime for Hyper-K. The neutrino-oxygen cross section, σ , is taken from GENIE 3.2.0 using tune G18.10a.02_11b, which is based on a local Fermi-gas model and an empirical meson-exchange model [83–85]. Here, we use the neutrino-oxygen cross section as an approximation for the total neutrino-water cross section. For neutrino energies between 100 MeV and 10 GeV, we predict $\sim 62,000 \nu_e$ and $\sim 110,000 \nu_\mu$ events, agreeing well with the predictions of [86] when scaled to Super-K. *This implies that Hyper-K’s statistical uncertainty is below 1%*. As a result, Hyper-K has the statistical power to distinguish between the different cosmic-ray models, which can differ by up to 20%.

Figure 2 shows the resulting neutrino count ratios (compared to an AMS injection) for the ν_e CC channel when injecting the different primary CR models and measurements. Note that the shape of the neutrino spectrum changes depending on energy for the different injections. *This shows that a flat scaling cannot capture the energy-dependent uncertainty of the primary flux.* This will become particularly relevant once future experiments reach $\sim 5\%$ statistical precision.

To illustrate the effect of using different primary cosmic ray spectra we first perform a simple analysis which focuses on the resulting shape of the atmospheric neutrino spectrum. We define the test statistic, q , as a maximum likelihood ratio, where the Poissonian likelihood is

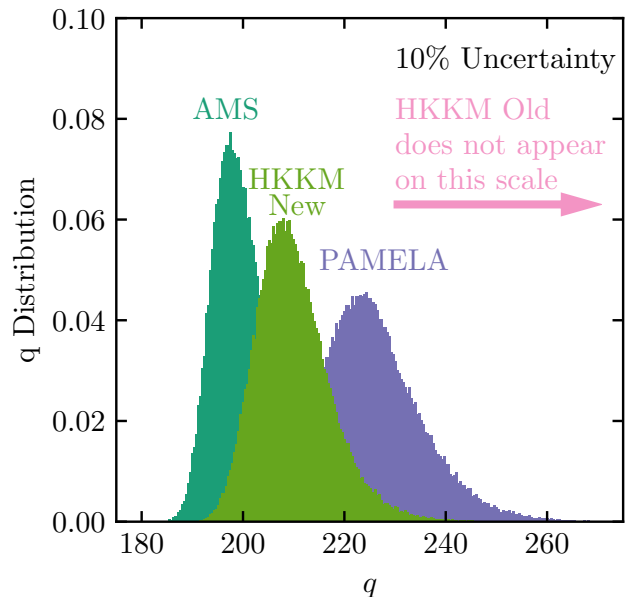


FIG. 3. Distribution of the test statistic for the primary CR models (holding the interaction model fixed) and accounting for a 10% cross-section uncertainty in the CC oxygen channel.

maximized with respect to two nuisance parameters: the overall normalization (taken as a free parameter) and the CC cross section (taken to be Gaussian with 10% uncertainty). We run the analysis for two distinct channels simultaneously: CC ν_e and CC ν_μ .

Figure 3 shows the resulting distribution of the test statistic when injecting different primary cosmic ray fluxes. The differences arise for multiple reasons: The large difference between the old HKKM model and AMS data arises at high energies, where changes in the spectral shape of the cosmic ray flux were not accounted for. PAMELA measurements are consistently higher than AMS measurements and show the most significant differences at ~ 700 GeV. The new HKKM model interpolates between low-energy data (AMS) and higher-energy measurements (CREAM, JACEE, and RUNJOB). This causes the HKKM model to lie slightly above the AMS measurements starting at a few 100 GeV. Not shown are measurements by other experiments, such as older AMS measurements [87], ATIC-2 [88], and BESS-TeV [89]. These differ more than PAMELA from AMS and would result in more significant changes in the test statistic.

From these distributions, we can extract the expected sensitivity of Hyper-K to the injected cosmic-ray fluxes using 10 years of data. For HKKM New, PAMELA, and HKKM Old, we predict sensitivities of 1.1σ , 2.1σ , and $\geq 5\sigma$, respectively, relative to the baseline fluxes using AMS data. By changing the energy range analyzed to $E_\nu \in [1 \text{ GeV}, 10 \text{ GeV}]$ we can slightly increase the sensitivity to the differences between AMS data and the model used in HKKM New to 1.4σ . These results point to two facts: *Hyper-K will be sensitive to the differences measured by cosmic-ray experiments and Hyper-K will even*

be sensitive to the interpolation between low-energy and high-energy cosmic-ray data.

Using the 10% uncertainty on the neutrino-nucleus cross section assumed here, there is no sensitivity to the helium component of the cosmic-rays. Should the uncertainty be reduced to 3%, Hyper-K would start to become sensitive to the measured helium flux. Note that this should be treated as a conservative statement, since we assume that helium and protons produce the same neutrino spectrum.

V. COSMIC RAY MODEL

Using the above results, we can then ask the question: *Can Hyper-K use its data to improve the cosmic-ray model?*

To this end, we reverse the analysis, reconstructing the primary spectrum based on all-sky ν_e and ν_μ measurements using the following procedure: First, we inject single proton lines at seven different energies and, following the same procedure as in the previous section, construct the resulting neutrino flux templates. We then use these seven neutrino spectra to fit the predicted Hyper-K all-sky measurement, binned as ten logarithmically spaced bins per decade in energy, using a χ^2 . In the fit, we include a systematic uncertainty on the neutrino-oxygen cross section of 10%. Note that we are free to increase or decrease the number of injected lines (templates). However, increasing the template count increases the uncertainty for each proton line, since there are large degeneracies between the resulting neutrino spectra from each line. Additionally, decreasing the number of templates makes reproducing the neutrino spectrum's shape more challenging.

Figure 4 shows the resulting fit. Each colored curve represents a neutrino flux template from a single injected CR proton line with a given energy. The resulting uncertainty on the reconstructed spectrum ranges from 5% to 10%, depending on the energy. *The main benefit of this analysis is reducing the uncertainty on the neutrino fluxes from 15% - 25% [90] to 5% - 10%*. Interestingly, this is similar to the best-fit values of the uncertainty on the flux normalization Super-K finds: for $E_\nu < 1$ GeV: 14.3% and for $E_\nu > 1$ GeV: 7.8% [90].

Figure 5 compares the fitted CR spectra for different injections to an AMS injection. Included are the resulting uncertainties on the fit of each CR energy bin. Of particular interest here is that the uncertainties and resulting fit values are *energy dependent*. This is of particular interest to studies that probe specific neutrino energies, such as oscillation studies.

VI. EFFECTS ON OSCILLATION STUDIES

A reduction in the uncertainty of the cosmic ray spectrum will have important implications for measuring neu-

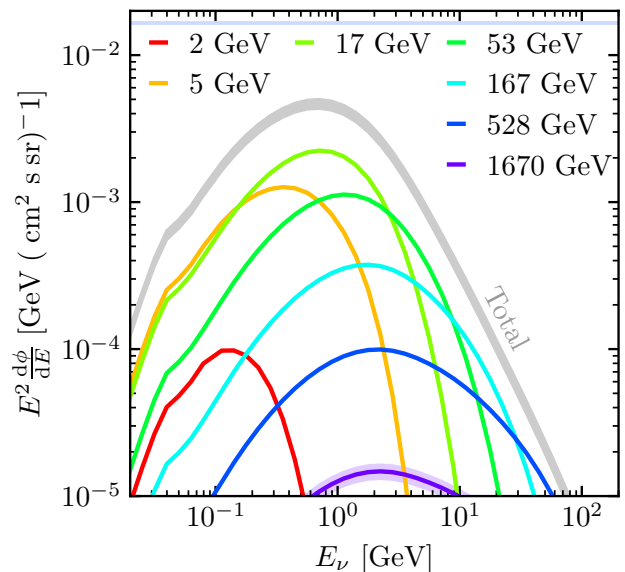


FIG. 4. Fitted neutrino spectrum, for discrete primary injections. Here, we fit 1900 kton-years worth of data. The shaded bands denote the uncertainty on each respective fit. Here we include a 10% systematic uncertainty on the neutrino-oxygen cross section.

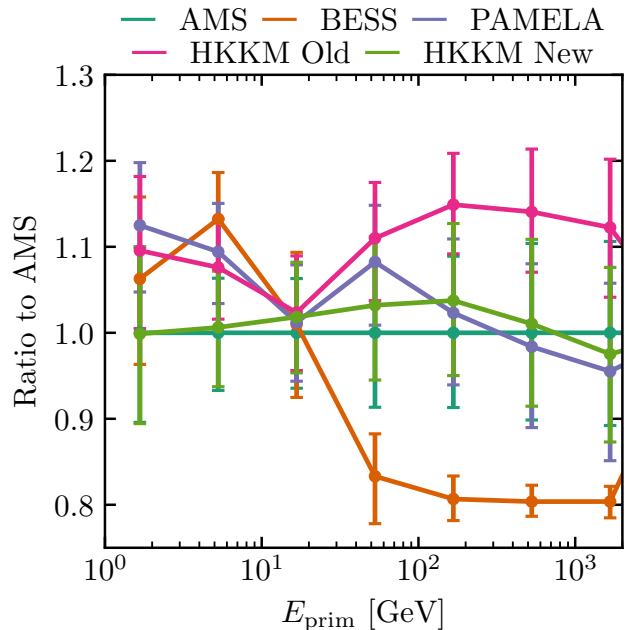


FIG. 5. The unfolded CR spectra based on predicted Hyper-K measurements for different injected fluxes.

trino mixing parameters. Here we explore this and show the effects that reduced cosmic ray uncertainties would have on a simplified $\sin^2 \theta_{23}$ study. This is meant to be considered a purely illustrative case, and may be extended with a more in-depth analysis.

We first construct oscillograms using `nuCraft` [91], and then fold them with the fitted neutrino spectra from the previous section. Using Equation 1, we then predict the

number of events per energy and angle bin, and compare the results for the different choice of neutrino parameters. Since we are comparing absolute counts in the analysis region between different $\sin^2 \theta_{23}$ hypotheses, the result is susceptible to the uncertainty on the overall normalization of the neutrino flux caused by the cross-section and primary model.

For illustrative purposes Fig. 6 shows the fractional difference in the expected number of counts in the ν_e CC channel considering two values of $\sin^2 \theta_{23}$. We choose the values $\sin^2 \theta_{23} = 0.45$ and 0.51 , which represent the best fit and boundary of the 1σ experimental uncertainty, respectively. The white circle in Figure 6 indicates our approximate analysis region, which focuses on the region most sensitive to changes in θ_{23} . For this example we predict a change of $\sim 12\%$ in total counts in the analysis region. However, distinguishing between these two θ_{23} values is only possible if the total normalization uncertainty is below 12% . Assuming a cross section uncertainty of 10% , we therefore require the neutrino flux uncertainty be below 7% (root-squared errors) to make such a distinction. As shown in the previous section, Hyper-K will be able to achieve this.

Moving beyond the illustrative example, we now wish to determine Hyper-K's sensitivity to θ_{23} using the improved primary CR model. To do this we generate 10^6 sample oscillograms for both the ν_e and the ν_μ CC channels, each including a 10% cross-section uncertainty. We perform a Poissonian likelihood analysis with an energy-dependent Gaussian nuisance parameter, which captures the cross-section and primary CR uncertainties. Additionally, we maximize the likelihood across energy and angle bins, resulting in the approximate region shown in Figure 6. Finally, 1σ confidence intervals for $\sin^2 \theta_{23}$ are determined keeping all other oscillation parameters constant.

We run the analysis using three CR uncertainty benchmarks: 15% (present value, as used by Super-K [90]), 7% (achievable value, as demonstrated in the previous section), and 0% (the ideal case). We find that using the present uncertainty value of 15% , $\sin^2 \theta_{23}$ is determined to be $0.45_{-0.046}^{+0.61}$ which does not improve upon the current measurement despite the increased statistics (i.e. it is systematics limited). However, for the 7% uncertainty case, $0.45_{-0.022}^{+0.29}$ is achievable, 50% - 73% of the uncertainty in Super-K's $\sin^2 \theta_{23}$ measurement [50]. This can be contrasted with the ideal case, which shows that ultimately θ_{23} can be known to $\leq 1\%$ precision if uncertainties in the CR spectrum are negligible. This is a surprising result, given the remaining systematic uncertainties (from the cross section) are 10% . However, since θ_{23} causes energy dependent changes in the neutrino spectrum, unlike the systematics, it can be determined to higher precision.

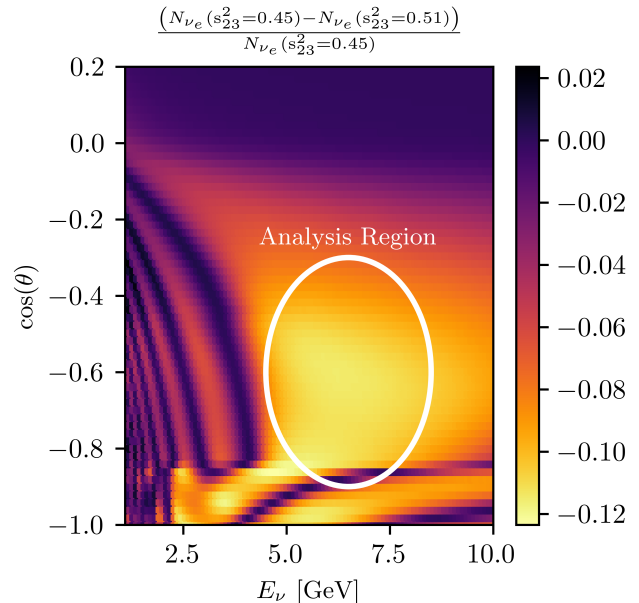


FIG. 6. Oscillogram showing the differences between the expected ν_e counts for $\sin^2 \theta_{23} = 0.45$ and 0.51 . The white circle indicates the approximate analysis region used in this study.

VII. CONCLUSION AND OUTLOOK

We have shown that next-generation kiloton-scale neutrino detectors, such as Hyper-Kamiokande, can provide a powerful new probe of the primary cosmic ray spectrum. While not designed as cosmic ray experiments, these detectors offer full-sky coverage, long-term stability, and unique sensitivity to low-energy features inaccessible to traditional satellite and balloon missions.

Hyper-Kamiokande can distinguish between leading cosmic ray models with high significance and reconstruct the primary spectrum to reduce flux uncertainties from $\sim 20\%$ to $\sim 7\%$. This improvement will directly enhance the precision of neutrino oscillation measurements, particularly in parameters such as $\sin^2 \theta_{23}$, and sharpen searches for diffuse supernova neutrinos, proton decay, and dark matter.

While the analysis in this paper has focused on the example of Hyper-Kamiokande as a proof of principle, a similar analysis should be possible for JUNO and DUNE. Looking forward with currently-operating experiments, complementary data from detectors like ORCA [13] and seasonal muon variations observed by BOREXINO [92], Super-K [93], IceCube [94–96], KM3NeT [97], and AUGER [98] offer promising paths to constrain cosmic ray uncertainties further. Our results emphasize that accounting for and reducing cosmic ray systematics will be critical for the next era of precision neutrino physics.

ACKNOWLEDGEMENTS

We are grateful for helpful discussions with John Beacom and Yi Zhuang. This work was supported by the Australian Research Council through Discovery Project DP220101727 plus the University of Melbourne’s Research Computing Services and the Petascale Campus Initiative. J.L.N was supported by the ARC Centre of Excellence for Dark Matter Particle Physics, CE200100008. L.E.S. acknowledges support from DOE Grant de-sc0010813. This work is based on the ideas and calculations of the authors, plus publicly available information.

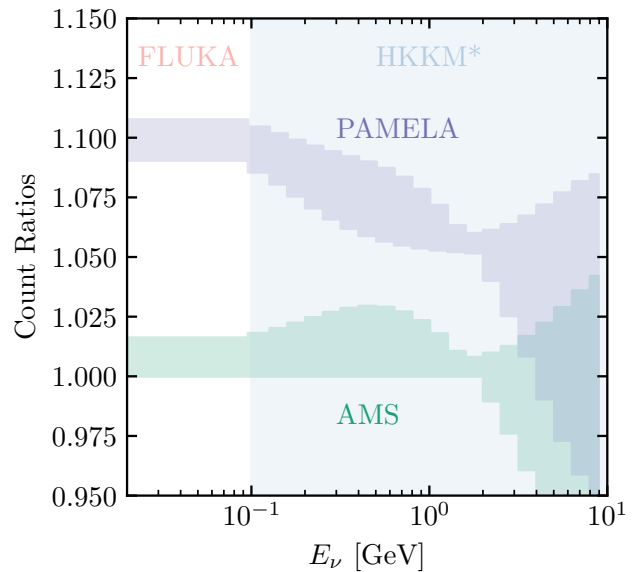


FIG. A.1. The count ratios including uncertainties from the interaction models. We also denote the relevant energy regions in our simulation. The lack of change at low energies is due to using FLUKA for all simulations.

Appendices

Appendix A: Interaction models

In the following we show the uncertainty bands caused by using different hadronic interaction models. To this end we inject either AMS or PAMELA data and generate neutrino spectra using Sybill 2.3 [68, 69], EPOS-LHC [70], QGSJET-II [71], and DPMJET-III [72, 73] and use those results to rescale the HKKM predictions.

* stephan.meighenberger@unimelb.edu.au

† jnewstead@unimelb.edu.au

‡ strigari@tamu.edu

- [1] F. An *et al.* (JUNO), Neutrino Physics with JUNO, *J. Phys. G* **43**, 030401 (2016), [arXiv:1507.05613](https://arxiv.org/abs/1507.05613) [physics.ins-det].
- [2] K. Abe *et al.* (Hyper-Kamiokande), Hyper-Kamiokande Design Report (2018), [arXiv:1805.04163](https://arxiv.org/abs/1805.04163) [physics.ins-det].
- [3] B. Abi *et al.* (DUNE), Deep Underground Neutrino Experiment (DUNE), Far Detector Technical Design Report, Volume IV: Far Detector Single-phase Technology, *JINST* **15** (08), T08010, [arXiv:2002.03010](https://arxiv.org/abs/2002.03010) [physics.ins-det].
- [4] J. Aalbers *et al.*, A next-generation liquid xenon observatory for dark matter and neutrino physics, *J. Phys. G* **50**, 013001 (2023), [arXiv:2203.02309](https://arxiv.org/abs/2203.02309) [physics.ins-det].
- [5] M. Aglietta *et al.* (NUSEX), Experimental study of atmospheric neutrino flux in the NUSEX experiment, *EPL* **8**, 611 (1989).
- [6] R. Becker-Szendy *et al.*, The Electron-neutrino and muon-neutrino content of the atmospheric flux, *Phys. Rev. D* **46**, 3720 (1992).
- [7] W. W. M. Allison *et al.* (Soudan 2), Measurement of the L/E distributions of atmospheric neutrinos in Soudan 2 and their interpretation as neutrino oscillations, *Phys. Rev. D* **68**, 113004 (2003), [arXiv:hep-ex/0307069](https://arxiv.org/abs/hep-ex/0307069).
- [8] M. C. Gonzalez-Garcia, M. Maltoni, and J. Rojo, Determination of the atmospheric neutrino fluxes from atmospheric neutrino data, *JHEP* **10**, 075, [arXiv:hep-ph/0607324](https://arxiv.org/abs/hep-ph/0607324).
- [9] R. Wendell *et al.* (Super-Kamiokande), Atmospheric neutrino oscillation analysis with sub-leading effects in Super-Kamiokande I, II, and III, *Phys. Rev. D* **81**, 092004 (2010), [arXiv:1002.3471](https://arxiv.org/abs/1002.3471) [hep-ex].
- [10] R. Abbasi *et al.* (IceCube), Measurement of the atmospheric neutrino energy spectrum from 100 GeV to 400 TeV with IceCube, *Phys. Rev. D* **83**, 012001 (2011), [arXiv:1010.3980](https://arxiv.org/abs/1010.3980) [astro-ph.HE].
- [11] M. G. Aartsen *et al.* (IceCube), Measurement of the Atmospheric ν_e flux in IceCube, *Phys. Rev. Lett.* **110**, 151105 (2013), [arXiv:1212.4760](https://arxiv.org/abs/1212.4760) [hep-ex].
- [12] Y. Fukuda *et al.* (Super-Kamiokande), Evidence for oscillation of atmospheric neutrinos, *Phys. Rev. Lett.* **81**, 1562 (1998), [arXiv:hep-ex/9807003](https://arxiv.org/abs/hep-ex/9807003).
- [13] S. Adrian-Martinez *et al.* (KM3Net), Letter of intent for KM3NeT 2.0, *J. Phys. G* **43**, 084001 (2016), [arXiv:1601.07459](https://arxiv.org/abs/1601.07459) [astro-ph.IM].
- [14] Z. Li *et al.* (Super-Kamiokande), Measurement of the tau neutrino cross section in atmospheric neutrino oscillations with Super-Kamiokande, *Phys. Rev. D* **98**, 052006 (2018), [arXiv:1711.09436](https://arxiv.org/abs/1711.09436) [hep-ex].
- [15] M. G. Aartsen *et al.* (IceCube), Measurement of Atmospheric Tau Neutrino Appearance with IceCube DeepCore, *Phys. Rev. D* **99**, 032007 (2019), [arXiv:1901.05366](https://arxiv.org/abs/1901.05366) [hep-ex].
- [16] I. Esteban, M. C. Gonzalez-Garcia, M. Maltoni, T. Schwetz, and A. Zhou, The fate of hints: updated global analysis of three-flavor neutrino oscillations, *JHEP* **09**, 178, [arXiv:2007.14792](https://arxiv.org/abs/2007.14792) [hep-ph].
- [17] S. A. Meighen-Berger, J. F. Beacom, N. F. Bell, and M. J. Dolan, New signal of atmospheric tau neutrino appearance: Sub-GeV neutral-current interactions in JUNO, *Phys. Rev. D* **109**, 092006 (2024), [arXiv:2311.01667](https://arxiv.org/abs/2311.01667) [hep-ph].
- [18] M. G. Aartsen *et al.* (IceCube-Gen2), Combined sensitivity to the neutrino mass ordering with JUNO, the IceCube Upgrade, and PINGU, *Phys. Rev. D* **101**, 032006 (2020), [arXiv:1911.06745](https://arxiv.org/abs/1911.06745) [hep-ex].
- [19] S. Aiello *et al.* (KM3NeT), Determining the neutrino mass ordering and oscillation parameters with KM3NeT/ORCA, *Eur. Phys. J. C* **82**, 26 (2022), [arXiv:2103.09885](https://arxiv.org/abs/2103.09885) [hep-ex].
- [20] Y. Fukuda *et al.* (Kamiokande), Atmospheric muon-neutrino / electron-neutrino ratio in the multiGeV energy range, *Phys. Lett. B* **335**, 237 (1994).
- [21] Y. Fukuda *et al.* (Super-Kamiokande), Measurement of a small atmospheric muon-neutrino / electron-neutrino ratio, *Phys. Lett. B* **433**, 9 (1998), [arXiv:hep-ex/9803006](https://arxiv.org/abs/hep-ex/9803006).
- [22] S. Horiuchi, J. F. Beacom, and E. Dwek, The Diffuse Supernova Neutrino Background is detectable in Super-Kamiokande, *Phys. Rev. D* **79**, 083013 (2009), [arXiv:0812.3157](https://arxiv.org/abs/0812.3157) [astro-ph].
- [23] J. F. Beacom, The Diffuse Supernova Neutrino Background, *Ann. Rev. Nucl. Part. Sci.* **60**, 439 (2010), [arXiv:1004.3311](https://arxiv.org/abs/1004.3311) [astro-ph.HE].
- [24] A. Gando *et al.* (KamLAND), A study of extraterrestrial antineutrino sources with the KamLAND detector, *Astrophys. J.* **745**, 193 (2012), [arXiv:1105.3516](https://arxiv.org/abs/1105.3516) [astro-ph.HE].
- [25] K. Abe *et al.* (Super-Kamiokande), Diffuse supernova neutrino background search at Super-Kamiokande, *Phys. Rev. D* **104**, 122002 (2021), [arXiv:2109.11174](https://arxiv.org/abs/2109.11174) [astro-ph.HE].
- [26] S. Abe *et al.* (KamLAND), Precision Measurement of Neutrino Oscillation Parameters with KamLAND, *Phys. Rev. Lett.* **100**, 221803 (2008), [arXiv:0801.4589](https://arxiv.org/abs/0801.4589) [hep-ex].
- [27] K. Abe *et al.* (Super-Kamiokande), Search for proton decay via $p \rightarrow e^+ \pi^0$ and $p \rightarrow \mu^+ \pi^0$ in 0.31 megaton-years exposure of the Super-Kamiokande water Cherenkov detector, *Phys. Rev. D* **95**, 012004 (2017), [arXiv:1610.03597](https://arxiv.org/abs/1610.03597) [hep-ex].
- [28] B. Abi *et al.* (DUNE), Deep Underground Neutrino Experiment (DUNE), Far Detector Technical Design Report, Volume II: DUNE Physics (2020), [arXiv:2002.03005](https://arxiv.org/abs/2002.03005) [hep-ex].
- [29] A. Olivares-Del Campo, C. Boehm, S. Palomares-Ruiz, and S. Pascoli, Dark matter-neutrino interactions through the lens of their cosmological implications, *Phys. Rev. D* **97**, 075039 (2018), [arXiv:1711.05283](https://arxiv.org/abs/1711.05283) [hep-ph].
- [30] C. A. Argüelles, A. Diaz, A. Kheirandish, A. Olivares-Del-Campo, I. Safa, and A. C. Vincent, Dark matter annihilation to neutrinos, *Rev. Mod. Phys.* **93**, 035007 (2021), [arXiv:1912.09486](https://arxiv.org/abs/1912.09486) [hep-ph].
- [31] K. Abe *et al.* (Super-Kamiokande), Indirect search for dark matter from the Galactic Center and halo with the Super-Kamiokande detector, *Phys. Rev. D* **102**, 072002 (2020), [arXiv:2005.05109](https://arxiv.org/abs/2005.05109) [hep-ex].
- [32] N. F. Bell, M. J. Dolan, and S. Robles, Dark matter pollution in the Diffuse Supernova Neutrino Background, *JCAP* **11**, 060, [arXiv:2205.14123](https://arxiv.org/abs/2205.14123) [hep-ph].

- [33] L. E. Strigari, Neutrino Coherent Scattering Rates at Direct Dark Matter Detectors, *New J. Phys.* **11**, 105011 (2009), [arXiv:0903.3630 \[astro-ph.CO\]](#).
- [34] J. Billard, L. Strigari, and E. Figueroa-Feliciano, Implication of neutrino backgrounds on the reach of next generation dark matter direct detection experiments, *Phys. Rev. D* **89**, 023524 (2014), [arXiv:1307.5458 \[hep-ph\]](#).
- [35] C. A. J. O'Hare, New Definition of the Neutrino Floor for Direct Dark Matter Searches, *Phys. Rev. Lett.* **127**, 251802 (2021), [arXiv:2109.03116 \[hep-ph\]](#).
- [36] M. Aguilar *et al.* (AMS), Precision Measurement of the Proton Flux in Primary Cosmic Rays from Rigidity 1 GV to 1.8 TV with the Alpha Magnetic Spectrometer on the International Space Station, *Phys. Rev. Lett.* **114**, 171103 (2015).
- [37] Y. S. Yoon *et al.*, Cosmic-Ray Proton and Helium Spectra from the First CREAM Flight, *Astrophys. J.* **728**, 122 (2011), [arXiv:1102.2575 \[astro-ph.HE\]](#).
- [38] O. Adriani *et al.* (PAMELA), PAMELA Measurements of Cosmic-ray Proton and Helium Spectra, *Science* **332**, 69 (2011), [arXiv:1103.4055 \[astro-ph.HE\]](#).
- [39] K. Abe *et al.*, Measurements of cosmic-ray proton and helium spectra from the BESS-Polar long-duration balloon flights over Antarctica, *Astrophys. J.* **822**, 65 (2016), [arXiv:1506.01267 \[astro-ph.HE\]](#).
- [40] M. Aguilar *et al.* (AMS), Precision Measurement of the Helium Flux in Primary Cosmic Rays of Rigidities 1.9 GV to 3 TV with the Alpha Magnetic Spectrometer on the International Space Station, *Phys. Rev. Lett.* **115**, 211101 (2015).
- [41] A. D. Panov *et al.*, Energy Spectra of Abundant Nuclei of Primary Cosmic Rays from the Data of ATIC-2 Experiment: Final Results, *Bull. Russ. Acad. Sci. Phys.* **73**, 564 (2009), [arXiv:1101.3246 \[astro-ph.HE\]](#).
- [42] T. K. Gaisser, Spectrum of cosmic-ray nucleons, kaon production, and the atmospheric muon charge ratio, *Astropart. Phys.* **35**, 801 (2012), [arXiv:1111.6675 \[astro-ph.HE\]](#).
- [43] T. K. Gaisser, T. Stanev, and S. Tilav, Cosmic Ray Energy Spectrum from Measurements of Air Showers, *Front. Phys. (Beijing)* **8**, 748 (2013), [arXiv:1303.3565 \[astro-ph.HE\]](#).
- [44] M. Honda, Atmospheric Neutrino Flux Calculation with NRLMSISE-00 Atmosphere Model and New Cosmic Ray Observations, *JPS Conf. Proc.* **12**, 010008 (2016).
- [45] M. Honda, T. Kajita, K. Kasahara, and S. Midorikawa, Improvement of low energy atmospheric neutrino flux calculation using the jam nuclear interaction model, *Physical Review D* **83**, 123001 (2011).
- [46] D. Heck, J. Knapp, J. N. Capdevielle, G. Schatz, and T. Thouw, CORSIKA: A Monte Carlo code to simulate extensive air showers (1998).
- [47] A. Fedynitch, R. Engel, T. K. Gaisser, F. Riehn, and T. Stanev, Calculation of conventional and prompt lepton fluxes at very high energy, *EPJ Web Conf.* **99**, 08001 (2015), [arXiv:1503.00544 \[hep-ph\]](#).
- [48] J. Evans, D. G. Gamez, S. D. Porzio, S. Söldner-Rembold, and S. Wren, Uncertainties in Atmospheric Muon-Neutrino Fluxes Arising from Cosmic-Ray Primaries, *Phys. Rev. D* **95**, 023012 (2017), [arXiv:1612.03219 \[astro-ph.HE\]](#).
- [49] H. Moraal, Cosmic-Ray Modulation Equations, *Space Sci. Rev.* **176**, 299 (2013).
- [50] T. Wester *et al.* (Super-Kamiokande), Atmospheric neutrino oscillation analysis with neutron tagging and an expanded fiducial volume in Super-Kamiokande I–V, *Phys. Rev. D* **109**, 072014 (2024), [arXiv:2311.05105 \[hep-ex\]](#).
- [51] Y. Zhuang, L. E. Strigari, and R. F. Lang, Time variation of the atmospheric neutrino flux at dark matter detectors, *Phys. Rev. D* **105**, 043001 (2022), [arXiv:2110.14723 \[hep-ph\]](#).
- [52] K. J. Kelly, P. A. N. Machado, N. Mishra, L. E. Strigari, and Y. Zhuang, Solar cycle effects in future measurements of low-energy atmospheric neutrinos, *Phys. Rev. D* **108**, 123019 (2023), [arXiv:2304.04689 \[hep-ph\]](#).
- [53] S. Buitink *et al.*, Performance of SKA as an air shower observatory, *PoS ICRC2021*, 415 (2021).
- [54] B. Flaggs, A. Coleman, and F. G. Schröder, Studying the mass sensitivity of air-shower observables using simulated cosmic rays, *Phys. Rev. D* **109**, 042002 (2024), [arXiv:2306.13246 \[hep-ph\]](#).
- [55] K. Asakimori, T. H. Burnett, M. L. Cherry, K. Chebli, M. J. Christ, S. Dake, J. H. Derrickson, W. F. Fountain, M. Fuki, J. C. Gregory, T. Hayashi, R. Holynski, J. Iwai, A. Iyono, J. Johnson, M. Kobayashi, J. Lord, O. Miyamura, K. H. Moon, B. S. Nilsen, H. Oda, T. Ogata, E. D. Olson, T. A. Parnell, F. E. Roberts, K. Sengupta, T. Shiina, S. C. Strausz, T. Sugitate, Y. Takahashi, T. Tominaga, J. W. Watts, J. P. Wefel, B. Wilczynska, H. Wilczynski, R. J. Wilkes, W. Wolter, H. Yokomi, and E. Zager, Cosmic-ray proton and helium spectra: Results from the jacee experiment, *The Astrophysical Journal* **502**, 278 (1998).
- [56] A. V. Apanasenko *et al.* (RUNJOB), Composition and energy spectra of cosmic ray primaries in the energy range 10^{13} -eV/particle to approximately 10^{15} -eV/particle observed by Japanese Russian joint balloon experiment, *Astropart. Phys.* **16**, 13 (2001).
- [57] T. K. Gaisser, R. Engel, and E. Resconi, *Cosmic rays and particle physics* (Cambridge University Press, 2016).
- [58] J. Matthews, A Heitler model of extensive air showers, *Astropart. Phys.* **22**, 387 (2005).
- [59] R. Engel, D. Heck, and T. Pierog, Extensive air showers and hadronic interactions at high energy, *Ann. Rev. Nucl. Part. Sci.* **61**, 467 (2011).
- [60] P. G. Edwards, R. J. Protheroe, and E. Rawinski, The muon component of gamma-ray-initiated air showers, *Journal of Physics G: Nuclear Physics* **11**, L101 (1985).
- [61] H. Dembinski *et al.*, The Muon Puzzle in air showers and its connection to the LHC, *PoS ICRC2021*, 037 (2021).
- [62] L. Cazon, R. Conceição, and F. Riehn, Universality of the muon component of extensive air showers, *JCAP* **03**, 022, [arXiv:2210.13407 \[hep-ph\]](#).
- [63] E. Richard *et al.* (Super-Kamiokande), Measurements of the atmospheric neutrino flux by Super-Kamiokande: energy spectra, geomagnetic effects, and solar modulation, *Phys. Rev. D* **94**, 052001 (2016), [arXiv:1510.08127 \[hep-ex\]](#).
- [64] G. Battistoni, A. Ferrari, T. Montaruli, and P. R. Sala, The atmospheric neutrino flux below 100-MeV: The FLUKA results, *Astropart. Phys.* **23**, 526 (2005).
- [65] P. Lipari, Lepton spectra in the earth's atmosphere, *Astropart. Phys.* **1**, 195 (1993).
- [66] G. Bossard, H. J. Drescher, N. N. Kalmykov, S. Ostapchenko, A. I. Pavlov, T. Pierog, E. A. Vishnevskaya, and K. Werner, Cosmic ray air shower characteristics in the framework of the parton based Gribov-

- Regge model NEXUS, *Phys. Rev. D* **63**, 054030 (2001), [arXiv:hep-ph/0009119](#).
- [67] T. Bergmann, R. Engel, D. Heck, N. N. Kalmykov, S. Ostapchenko, T. Pierog, T. Thouw, and K. Werner, One-dimensional Hybrid Approach to Extensive Air Shower Simulation, *Astropart. Phys.* **26**, 420 (2007), [arXiv:astro-ph/0606564](#).
- [68] F. Riehn, H. P. Dembinski, R. Engel, A. Fedynitch, T. K. Gaisser, and T. Stanev, The hadronic interaction model SIBYLL 2.3c and Feynman scaling, *PoS ICRC2017*, 301 (2018), [arXiv:1709.07227 \[hep-ph\]](#).
- [69] F. Riehn, R. Engel, A. Fedynitch, T. K. Gaisser, and T. Stanev, Hadronic interaction model Sibyll 2.3d and extensive air showers, *Phys. Rev. D* **102**, 063002 (2020), [arXiv:1912.03300 \[hep-ph\]](#).
- [70] T. Pierog, I. Karpenko, J. M. Katzy, E. Yatsenko, and K. Werner, EPOS LHC: Test of collective hadronization with data measured at the CERN Large Hadron Collider, *Phys. Rev. C* **92**, 034906 (2015), [arXiv:1306.0121 \[hep-ph\]](#).
- [71] S. Ostapchenko, Monte Carlo treatment of hadronic interactions in enhanced Pomeron scheme: I. QGSJET-II model, *Phys. Rev. D* **83**, 014018 (2011), [arXiv:1010.1869 \[hep-ph\]](#).
- [72] S. Roesler, R. Engel, and J. Ranft, The Monte Carlo event generator DPMJET-III, in *International Conference on Advanced Monte Carlo for Radiation Physics, Particle Transport Simulation and Applications (MC 2000)* (2000) pp. 1033–1038, [arXiv:hep-ph/0012252](#).
- [73] A. Fedynitch, *Cascade equations and hadronic interactions at very high energies*, Ph.D. thesis, KIT, Karlsruhe, Dept. Phys. (2015).
- [74] J. M. Picone, A. E. Hedin, D. P. Drob, and A. C. Aikin, NRLMSISE-00 empirical model of the atmosphere: Statistical comparisons and scientific issues, *Journal of Geophysical Research (Space Physics)* **107**, 1468 (2002).
- [75] A. Fedynitch and M. Huber, Data-driven hadronic interaction model for atmospheric lepton flux calculations, *Phys. Rev. D* **106**, 083018 (2022), [arXiv:2205.14766 \[astro-ph.HE\]](#).
- [76] M. Honda, T. Kajita, K. Kasahara, S. Midorikawa, and T. Sanuki, Calculation of atmospheric neutrino flux using the interaction model calibrated with atmospheric muon data, *Phys. Rev. D* **75**, 043006 (2007), [arXiv:astro-ph/0611418](#).
- [77] Y. Fukuda *et al.* (Super-Kamiokande), The Super-Kamiokande detector, *Nucl. Instrum. Meth. A* **501**, 418 (2003).
- [78] J. Bian *et al.* (Hyper-Kamiokande), Hyper-Kamiokande Experiment: A Snowmass White Paper, in *Snowmass 2021* (2022) [arXiv:2203.02029 \[hep-ex\]](#).
- [79] Y. Ashie *et al.* (Super-Kamiokande), A Measurement of atmospheric neutrino oscillation parameters by SUPER-KAMIOKANDE I, *Phys. Rev. D* **71**, 112005 (2005), [arXiv:hep-ex/0501064](#).
- [80] M. Shiozawa (Super-Kamiokande), Reconstruction algorithms in the Super-Kamiokande large water Cherenkov detector, *Nucl. Instrum. Meth. A* **433**, 240 (1999).
- [81] E. Drakopoulou, G. A. Cowan, M. D. Needham, S. Playfer, and M. Taani, Application of machine learning techniques to lepton energy reconstruction in water Cherenkov detectors, *JINST* **13** (04), P04009, [arXiv:1710.05668 \[physics.ins-det\]](#).
- [82] M. Jiang *et al.* (Super-Kamiokande), Atmospheric Neutrino Oscillation Analysis with Improved Event Reconstruction in Super-Kamiokande IV, *PTEP* **2019**, 053F01 (2019), [arXiv:1901.03230 \[hep-ex\]](#).
- [83] C. Andreopoulos *et al.*, The GENIE Neutrino Monte Carlo Generator, *Nucl. Instrum. Meth. A* **614**, 87 (2010), [arXiv:0905.2517 \[hep-ph\]](#).
- [84] C. Andreopoulos, C. Barry, S. Dytman, H. Gallagher, T. Golan, R. Hatcher, G. Perdue, and J. Yarba, The GENIE Neutrino Monte Carlo Generator: Physics and User Manual, (2015), [arXiv:1510.05494 \[hep-ph\]](#).
- [85] J. Tena-Vidal *et al.* (GENIE), Neutrino-nucleon cross-section model tuning in GENIE v3, *Phys. Rev. D* **104**, 072009 (2021), [arXiv:2104.09179 \[hep-ph\]](#).
- [86] B. Zhou and J. F. Beacom, First detailed calculation of atmospheric neutrino foregrounds to the diffuse supernova neutrino background in Super-Kamiokande, *Phys. Rev. D* **109**, 103003 (2024), [arXiv:2311.05675 \[hep-ph\]](#).
- [87] B. Alpat, The results of alpha magnetic spectrometer (ams) experiment in space, *Nuclear Physics B - Proceedings Supplements* **110**, 179 (2002).
- [88] A. D. Panov, J. H. Adams, H. S. Ahn, G. L. Bashinzhagyan, J. W. Watts, J. P. Wefel, J. Wu, O. Ganel, T. G. Guzik, V. I. Zatsepin, I. Isbert, K. C. Kim, M. Christl, E. N. Kouznetsov, M. I. Panasyuk, E. S. Seo, N. V. Sokolskaya, J. Chang, W. K. H. Schmidt, and A. R. Fazely, Energy spectra of abundant nuclei of primary cosmic rays from the data of ATIC-2 experiment: Final results, *Bulletin of the Russian Academy of Sciences, Physics* **73**, 564 (2009), [arXiv:1101.3246 \[astro-ph.HE\]](#).
- [89] S. Haino *et al.*, Measurements of primary and atmospheric cosmic - ray spectra with the BESS-TeV spectrometer, *Phys. Lett. B* **594**, 35 (2004), [arXiv:astro-ph/0403704](#).
- [90] K. Abe *et al.* (Super-Kamiokande), Atmospheric neutrino oscillation analysis with external constraints in Super-Kamiokande I-IV, *Phys. Rev. D* **97**, 072001 (2018), [arXiv:1710.09126 \[hep-ex\]](#).
- [91] M. Wallraff and C. Wiebusch, Calculation of oscillation probabilities of atmospheric neutrinos using nuCraft, *Comput. Phys. Commun.* **197**, 185 (2015), [arXiv:1409.1387 \[astro-ph.IM\]](#).
- [92] M. Agostini *et al.* (Borexino), Modulations of the Cosmic Muon Signal in Ten Years of Borexino Data, *JCAP* **02**, 046, [arXiv:1808.04207 \[hep-ex\]](#).
- [93] H. Kitagawa *et al.* (Super-Kamiokande), Measurements of the charge ratio and polarization of cosmic-ray muons with the Super-Kamiokande detector, *Phys. Rev. D* **110**, 082008 (2024), [arXiv:2403.08619 \[hep-ex\]](#).
- [94] M. G. Aartsen *et al.* (IceCube), Characterization of the Atmospheric Muon Flux in IceCube, *Astropart. Phys.* **78**, 1 (2016), [arXiv:1506.07981 \[astro-ph.HE\]](#).
- [95] *The IceCube Neutrino Observatory - Contributions to ICRC 2017 Part III: Cosmic Rays* (2017) [arXiv:1710.01194 \[astro-ph.HE\]](#).
- [96] S. Tilav, T. K. Gaisser, D. Soldin, and P. Desiati (IceCube), Seasonal variation of atmospheric muons in IceCube, *PoS ICRC2019*, 894 (2020), [arXiv:1909.01406 \[astro-ph.HE\]](#).
- [97] S. Aiello *et al.* (KM3NeT), Atmospheric muons measured with the KM3NeT detectors in comparison with updated numeric predictions, *Eur. Phys. J. C* **84**, 696 (2024), [arXiv:2403.11946 \[astro-ph.HE\]](#).

- [98] D. Góra (Pierre Auger), Muon measurements at the Pierre Auger Observatory, *SciPost Phys. Proc.* **15**, 020 (2024), [arXiv:2209.13392 \[astro-ph.HE\]](#).